

Second, the sterically hindered catalyst Mn(TMP)Cl exhibits substantial shape selectivity in the catalytic epoxidation of olefins, and this is shown to be directly attributable to the differences in binding energies for formation of the intermediate. Our observations suggest a strategy for the development of other shape-selective, as well as asymmetric, porphyrin catalysts for olefin epoxidation.

These findings in turn argue that the oxo-olefin complex does not contain carbon-based cationic or radicaloid centers. The formation of this complex is rather insensitive to electronic effects of the olefin, but it is markedly influenced by steric interactions when the more sterically demanding catalyst, Mn(TMP)Cl, is used. These conclusions are consistent with our postulate that the intermediate is a metallaoxetane, which we speculate is formed by a concerted antarafacial 2 + 2 cycloaddition.²⁹ On the basis of the evidence presented here, it appears the normal mode of decomposition of this species is a concerted reductive elimination. Complete substantiation of these postulates awaits direct structural and spectroscopic analysis of the intermediate. Such studies are currently being pursued in our laboratories.

Finally, these studies have shed light on the general reactivity of high-valent manganese oxo porphyrins. At this point, the possible extension of this mechanism to other metals is not proven,

but it seems plausible. In view of the similar reactivities of cytochrome P-450 and other model systems as evidenced by N and O demethylation,³⁰ the NIH shift,³¹ and alkane hydroxylation,³² it would not be surprising to find other similar stereoselective olefin epoxidations occurring by this general route.

Acknowledgment. Support from the National Institutes of Health (Grant NIH GM17880-13,14) is gratefully acknowledged. The Nicolet NMC-300 spectrometer was purchased with funds from the National Science Foundation (Grant NSF CHE81-09064 to Stanford University). Support for Teruyuki Hayashi from the Science and Technology Agency of Japan and for Scott Raybuck from the Franklin Veatch Memorial Fellowship is also gratefully acknowledged.

Registry No. Mn(TPP)Cl, 32195-55-4; Mn(TMP)Cl, 85939-49-7; lithium hypochlorite, 13840-33-0; cytochrome P-450, 9035-51-2; monooxygenase, 9038-14-6; cyclooctene, 931-88-4; (Z)-2-octene, 13389-42-9; indene, 95-13-6; 1-ethenylbenzene, 100-42-5; 1-methylcyclohex-1-ene, 591-49-1; (E)-1-propenylbenzene, 873-66-5; *trans,trans,cis*-1,5,9-cyclododecatriene, 706-31-0; *cis*-stilbene, 645-49-8; (Z)-1-propenylbenzene, 766-90-5; (E)-2-octene, 7642-04-8; (E)-4-octene, 14850-23-8; 1,3-cyclohexadiene, 592-57-4; 1,3-cycloheptadiene, 4054-38-0; 1,3-cyclooctadiene, 1700-10-3.

(28) Halpern, J. *Science* **1982**, *217*, 401-407 and references therein.

(29) The metallaoxetane species has also been considered by Groves as an intermediate in the FeTPPCl catalyzed oxygenation of cyclohexene with iodobenzene.^{8b}

(30) Shannon, P.; Bruce, T. C. *J. Am. Chem. Soc.* **1981**, *103*, 4580-4582.

(31) Lindsay-Smith, J. R.; Piggott, R. E.; Steath, P. R. *J. Chem. Soc., Chem. Commun.* **1982**, 55-56.

(32) Groves, J. T.; Subramanian, D. V. *J. Am. Chem. Soc.* **1984**, *106*, 2177-2181.

Homogeneous Catalysis of the Photoreduction of Water. 6. Mediation by Polypyridine Complexes of Ruthenium(II) and Cobalt(II) in Alkaline Media¹

C. V. Krishnan, Bruce S. Brunshwig, Carol Creutz,* and Norman Sutin*

Contribution from the Department of Chemistry, Brookhaven National Laboratory, Upton, New York 11973. Received August 13, 1984

Abstract: The emission of (polypyridine)ruthenium(II) complexes (S) is quenched by (polypyridine)cobalt(II) (CoL₃²⁺) complexes via parallel oxidative, reductive, and energy-transfer paths, giving CoL₃³⁺ + S⁺, CoL₃³⁺ + S⁻, and *CoL₃²⁺ + S, respectively. The oxidative route provides the basis for a new water photoreduction sequence: in mixed acetonitrile-water solvents relatively high cage-escape yields of Ru(4,7-(CH₃)₂phen)₃³⁺ and Co(bpy)₃³⁺ (S = Ru(4,7-(CH₃)₂phen)₃²⁺, phen = 1,10-phenanthroline, bpy = 2,2'-bipyridine) are obtained. The Ru(III) complex is reduced by triethanolamine (TEOA), and the Co(bpy)₃³⁺ reacts with water and/or TEOAH⁺ to give H₂. The maximum H₂ quantum yield obtained is 0.29 in 50% acetonitrile-water. Unusual features of the system are the fact that, at low TEOA, Co(bpy)₃²⁺ scavenging of Ru(III) reduces the H₂ yield and that the cage-escape and limiting H₂ yields are strongly solvent dependent: for the Ru(4,7-(CH₃)₂phen)₃²⁺-Co(bpy)₃²⁺-TEOA system the H₂ yield increases from ~0.02 in H₂O to 0.29 in the mixed solvent. Reduction potentials for CoL₃^{3+/2+} and CoL₃^{2+/+} couples are also reported.

Cobalt-polypyridine complexes are of interest in a number of contexts [L = polypyridine, i.e., 1,10-phenanthroline (phen) or 2,2'-bipyridine (bpy)]: the cobalt(I) complexes reduce water to H₂²⁻⁴ and CO₂ to CO⁵ depending upon conditions. Since the

cobalt(I) species may be generated by the reduction of the corresponding cobalt(II) or cobalt(III) species, catalytic systems incorporating this chemistry are possible. When RuL₃²⁺ complexes⁶⁻⁸ are used as sensitizers, cobalt(I) complexes may be generated either via reductive (eq 2) or oxidative (eq 3) quenching of the excited state in the presence of an electron donor (D).

(1) Part 5 in the series is ref 9a.

(2) Krishnan, C. V.; Sutin, N. *J. Am. Chem. Soc.* **1981**, *103*, 2141.

(3) Krishnan, C. V.; Creutz, C.; Mahajan, D.; Schwarz, H. A.; Sutin, N. *Isr. J. Chem.* **1982**, *22*, 98.

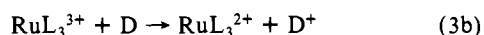
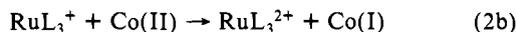
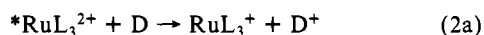
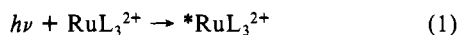
(4) Kirch, M.; Lehn, J.-M.; Sauvage, J. P. *Helv. Chim. Acta* **1979**, *62*, 1345.

(5) Lehn, J.-M.; Ziessel, R. *Proc. Natl. Acad. Sci. U.S.A.* **1982**, *79*, 701.

(6) Lin, C.-T.; Böttcher, W.; Chou, M.; Creutz, C.; Sutin, N. *J. Am. Chem. Soc.* **1976**, *98*, 6536.

(7) Sutin, N.; Creutz, C. *Adv. Chem. Ser.* **1978**, No. 168, 1.

(8) Sutin, N. *J. Photochem.* **1979**, *10*, 19.



In each case the net reaction is



In earlier work, we found that a homogeneous system employing cobalt(II)- and ruthenium(II)-polypyridine complexes effected the photoreduction of water to hydrogen at pH 4–5 with visible light.^{2,3} Ascorbate ion was the electron donor and reduced $* \text{RuL}_3^{2+}$ to RuL_3^+ (eq 2a); Co(bpy)_n^{2+} was reduced to Co(bpy)_n^+ by RuL_3^+ (eq 2b) and Co(I) reacted with water or H_3O^+ via a cobalt(III)-hydride⁹ to give H_2 . In the present work we have evaluated the rate constants for quenching of different (polypyridine)ruthenium(II) complexes by CoL^{2+} and CoL_3^{2+} as a function of L and found evidence that, depending on the sensitizer-quencher combination, reductive, oxidative, or energy-transfer quenching may predominate. For the combination $\text{Ru(4,7-(CH}_3)_2\text{phen)}_3^{2+}$ - Co(bpy)_3^{2+} a new photoreduction system based on oxidative quenching of the ruthenium(II) excited state has been characterized. In basic 50% aqueous acetonitrile with triethanolamine the electron donor in eq 3b, H_2 production is limited only by the efficiency of cage escape in the quenching reaction (eq 3a).

Experimental Section

Materials. The (polypyridine)ruthenium(II) complexes were prepared as in an earlier study.⁶ All the ligands were from G. F. Smith and Fisher and were used without further purification. Cobalt(II) sulfate was puratronic grade from Johnson Matthey. The solvents were of spectronic grade. The organic electron donors were from Aldrich and were used without further purification. The diquat dibromide and the tetraalkylammonium salts were from earlier studies.^{10,11}

Emission Intensity Measurement. The emission from the (polypyridine)ruthenium(II) complexes were measured as described previously.⁶ Solutions in 1×1 cm cells were deaerated for about 20 min with argon and then excited at the absorption maximum of the ruthenium(II) complex around 450 nm. The emission intensities were measured at ~ 600 – 630 nm in the energy mode. Neutral density filters were used to reduce the incident light intensity. Stern-Volmer constants ($K_{SV} = [I_0/I - 1]/[Q]$) were obtained from plots of the emission intensity data as a function of the concentration of the quencher, Q. For quenching by the cobalt-bipyridine complexes, the emission intensities at 610 nm were corrected for absorption of the incident excitation light at 450 nm. Quenching rate constants were calculated from $k_q = K_{SV}/\tau_0$, where τ_0 is the excited-state lifetime in the absence of added quencher.⁶

Cyclic Voltammetry. A Princeton Applied Research system consisting of a Model 173 potentiostat and a Model 175 universal programmer was employed in these studies. Sweep rates of 20–500 mV s^{-1} were used and the cyclic voltammograms were recorded on an x-y recorder. Most of the determinations were carried out in acetonitrile in a cell containing a platinum working electrode and a platinum wire auxiliary electrode. A saturated calomel electrode was used as the reference electrode. The solutions were deaerated with argon. For cobalt-bipyridine and related complexes a Co(II) :ligand ratio of 1:5 was used. Some measurements on cobalt(III) complexes were also performed. In addition, several of the CoL_3^{2+} or CoL_3^{3+} complexes were studied in aqueous media. In these experiments a glassy carbon electrode (PAR) was the working electrode and the medium was 0.16 M Na_2SO_4 containing 0.02 M 2-aminoethanol buffer (pH 9.6).

Continuous Photolysis. The photolysis system consisted of a 450-W xenon lamp, focusing lenses, UV cutoff filters, and a thermostated bath for the photolysis vessel. In the hydrogen generation studies 25-mL solutions were stirred continuously and irradiated in 2×2 cm square cells after deaerating for about 30 min with argon. The volume of gas pro-

duced was measured as a function of time by a volumeter attachment or analyzed on a Varian 1400 gas chromatograph. Light intensities were determined by $\text{Ru(bpy)}_3^{2+}/\text{Co(NH}_3)_5\text{Cl}^{2+}$ actinometry³ and were typically 3×10^{-5} einstein min^{-1} .

Flash Photolysis. The yield of separated electron-transfer products Y_d was determined by using a frequency-doubled Nd laser as excitation source.⁶ The absorbance changes occurring during and after the 25-ns 530-nm pulse were monitored at 420–450 nm and compared¹² with those produced in the RuL_3^{2+} - Fe^{3+} system in 0.5 M H_2SO_4 , which was assumed to produce separated RuL_3^{3+} and Fe^{2+} in 100% yield.

Rate constants for RuL_3^{3+} - Co(bpy)_3^{2+} and RuL_3^{3+} -TEOA reactions were determined by using a Phase-R Model DL-1100 dye laser as excitation source.¹² For both reactions the quenching of $* \text{RuL}_3^{2+}$ (0.1 mM) by Co(bpy)_3^{2+} (1 mM) was used to generate RuL_3^{3+} (and Co(bpy)_3^{2+}). The RuL_3^{3+} reduction was studied at 420–450 nm under pseudo-first-order conditions, with sufficient Co(bpy)_3^{2+} (0.2–0.6 mM) or TEOA (2–6 mM) being added so that the rate of the “primary” RuL_3^{3+} - Co(bpy)_3^{2+} back-reaction was negligible.

Results

Reduction potentials determined for $\text{CoL}_3^{3+/2+}$ couples in either acetonitrile or water are summarized in Table I. Peak separations $E_{pa} - E_{pc}$ were 70–110 mV, depending upon the sweep rate (20–200 mV/s) and the couple. Since all the systems were chemically reversible, the average of E_{pc} and E_{pa} is reported as $E_{1/2}$. Data for $\text{CoL}_3^{2+/+}$ couples in the two solvents are also included in the table. These couples were electrochemically well-behaved in acetonitrile, exhibiting equal currents for cathodic and anodic peaks and peak separations of 60–100 mV. In water, however, large anodic spikes 40–130-mV positive of E_{pc} were observed for all five complexes investigated. In addition, for the phen derivatives, the presence of excess L caused coating of the electrode during the -1 to -1.5 -V portion of the sweep. Thus the measurements were performed with 3:1 L:Co(II) ratios or with the CoL_3^{3+} complex. Frequent polishing of the carbon working electrode was essential. The numbers reported are obtained from E_{pc} (at 50 mV/s scan rate) but are not regarded as true $E_{1/2}$ values since the couples are not well-behaved in water and since the values (especially for the phen derivatives) do not change sufficiently with L. Thus the acetonitrile data are used in subsequent discussions.

Rate constants for quenching of $* \text{RuL}_3^{2+}$ emission by CoL^{2+} and CoL_3^{2+} complexes are presented in Tables II and III, respectively. In Table IV rate constants for the quenching of $* \text{RuL}_3^{2+}$ and $* \text{OsL}_3^{2+}$ emission by CoL_3^{2+} complexes are summarized. The dependence of k_q for CoL^{2+} , CoL_3^{2+} , and CoL_3^{3+} on the nature of supporting electrolyte anion is shown in Table V. Rate constants for quenching $* \text{Ru(4,4'-(CH}_3)_2\text{bpy)}_3^{2+}$ emission by diquat dibromide as a function of supporting electrolyte cation are listed in the supplementary material, Table I. Triethanolamine does not detectably quench Ru(bpy)_3^{2+} or $\text{Ru(4,7-(CH}_3)_2\text{phen)}_3^{2+}$ emission; i.e., for these sensitizers $k_q < 10^5 \text{ M}^{-1} \text{ s}^{-1}$.

Rate constants for reduction of RuL_3^{3+} by Co(bpy)_3^{2+} (determined by flash photolysis) are presented in Table VI. The rate constant for reduction of $\text{Ru(4,7-(CH}_3)_2\text{phen)}_3^{3+}$ by triethanolamine is $5.2 \times 10^6 \text{ M}^{-1} \text{ s}^{-1}$ at 25 °C in 50% aqueous acetonitrile containing 0.25 M LiCl.

Water Photoreduction. In preliminary experiments (supplementary material, Tables II–VIII) it was established that H_2 is produced from $\text{RuL}_3^{2+}/\text{CoL}_n^{2+}$ mixtures at pH > 7 only in the presence of rather high concentrations of Co(II) ($> 5 \times 10^{-3}$ M) and reducing agent. Among organic amines investigated as electron donors, triethanolamine (TEOA) was superior. The sensitizer $\text{Ru(4,7-(CH}_3)_2\text{phen)}_3^{2+}$ was effective in purely aqueous media (and the best in 50% aqueous acetonitrile) and found to be extremely stable under irradiation under both H_2 -generating and nongenerating conditions. Addition of acetonitrile to mixtures such as those used in the above experiments considerably increased the H_2 production rates (% CH_3CN by volume, relative H_2 production rate with 2.5×10^{-4} M $\text{Ru(4,7-(CH}_3)_2\text{phen)}_3^{2+}$, 0.01

(9) (a) Creutz, C.; Schwarz, H. A.; Sutin, N. *J. Am. Chem. Soc.* **1984**, *106*, 3036. (b) Schwarz, H. A.; Creutz, C.; Sutin, N. *Inorg. Chem.* **1985**, *24*, 433.

(10) Creutz, C.; Keller, A. D.; Sutin, N.; Zipp, A. P. *J. Am. Chem. Soc.* **1982**, *104*, 3618.

(11) Krishnan, C. V.; Friedman, H. J. *Phys. Chem.* **1969**, *73*, 3934.

(12) Mok, C.-Y.; Zanella, A. W.; Creutz, C.; Sutin, N. *Inorg. Chem.* **1984**, *23*, 2891.

Table I. Reduction Potentials $E_{1/2}$ (V) for $\text{CoL}_3^{3+/2+}$ and $\text{CoL}_3^{2+/+}$ Couples at $\sim 22^\circ\text{C}$

L	$\text{CoL}_3^{3+/2+}$		$\text{CoL}_3^{2+/+}$	
	$\text{CH}_3\text{CN}^{a,b}$	H_2O^a	$\text{CH}_3\text{CN}^{a,b}$	H_2O^b
bpy	0.30	0.30, ^c 0.304, ^d 0.30 ^e	-0.98	-0.89, ^f -0.95 ^g
4,4'-(CH_3) ₂ bpy	0.18	0.17, ^c 0.16 ^g	-1.10	-1.0, ^f -1.03 ^g
5-Clphen	0.48 ⁱ	0.50 ^g	-0.86 ⁱ	-0.82 ^g
phen	0.37	0.36, ^c 0.38, ^d 0.37 ^g	-0.96	$\sim -0.8,$ ^d -0.84 ^g
4,7-(CH_3) ₂ phen	0.18	0.19, ^c 0.26, ^d 0.17 ^g	-1.10	-0.82 ^g
2,9-(CH_3) ₂ phen ^j	0.6 ^e	0.6 ^{c,e}	-1.16	

^aThe average of E_{pa} and E_{pc} , determined at 20–200 mV s⁻¹ sweep rates. ^bMeasured in acetonitrile containing 0.1 M tetraethylammonium or tetrabutylammonium perchlorate; Pt working electrode, SCE reference electrode. ^cMeasured in aqueous 0.166 M Na_2SO_4 (0.01 M H_2SO_4) with a glassy carbon working electrode. Value vs. NHE. ^dFor 0.5 M H_2SO_4 , reported by: Chen, Y. W.; Santhanam, K. S. V.; Bard, A. J. *J. Electrochem. Soc.* **1982**, *129*, 61. ^e E_{pa} for CoL_3^{2+} ; irreversible. ^fReference 3, determined in carbonate buffer, vs. NHE. ^gMeasured with a glassy carbon working electrode in 0.16 M Na_2SO_4 containing 0.02 M 2-aminoethanol buffer, pH 9.6; vs. NHE. ^hLarge anodic current spikes are observed for all L reported. The number reported is calculated from E_{pc} measured at 50 mV s⁻¹ by using $E_{1/2} = E_{pc} + 0.03 + 0.242$ where 0.03 V assumes electrochemical reversibility ($\Delta E_p = 60$ mV) and 0.242 is the correction for the SCE reference electrode. ⁱMahajan, D.; Zanella, A. W., unpublished observations. ^jFor steric reasons, these complexes may have the formula CoL_2^{n+} rather than CoL_3^{n+} .

Table II. Rate Constants k_q ($\times 10^8$, $\text{M}^{-1} \text{s}^{-1}$) for the Quenching of (Polypyridine)ruthenium(II) Emission by CoL^{2+} at 25°C , 0.05 M Ionic Strength, and pH 6.0^a

L	sensitizer			
	$\text{Ru}(\text{bpy})_3^{2+}$	$\text{Ru}(5\text{-Clphen})_3^{2+}$	$\text{Ru}(\text{phen})_3^{2+}$	$\text{Ru}(4,7\text{-(CH}_3)_2(\text{phen})_3^{2+}$
5-Brphen				3.4
5-Clphen	0.23	1.7	1.9	2.8
phen	0.27	0.64	0.9	1.6
5-(CH_3)phen				2.0
5,6-(CH_3) ₂ phen				3.0
4,7-(CH_3) ₂ phen	0.7	2.4	2.7	4.3
2,9-(CH_3) ₂ phen				5.4
bpy	0.55	0.27	0.34	0.29
4,4'-(CH_3) ₂ bpy				0.74

^aCo(II):L is 4.54:1; 0.05 M phosphate buffer.

Table III. Rate Constants k_q ($\times 10^8$, $\text{M}^{-1} \text{s}^{-1}$) for the Quenching of (Polypyridine)ruthenium(II) Emission by CoL_3^{2+} at 25°C , ~ 0.075 M Ionic Strength, and pH 8.0^a

L	sensitizer			
	$\text{Ru}(\text{bpy})_3^{2+}$	$\text{Ru}(5\text{-Clphen})_3^{2+}$	$\text{Ru}(\text{phen})_3^{2+}$	$\text{Ru}(4,7\text{-(CH}_3)_2(\text{phen})_3^{2+}$
bpy	0.28	0.79	0.63	1.00
5-Clphen	0.63	1.25	1.24	1.36
phen	0.30	0.98	0.77	1.14
4,7-(CH_3) ₂ phen	0.74	1.20	1.05	1.39

^aCo(II):L is 1:5; 0.05 M phosphate buffer.

Table IV. $^*\text{ML}_3^{2+}$ Redox Potentials and Rate Constants for Quenching of ML_3^{2+} Emission by $\text{Co}(\text{bpy})_3^{2+}$ at 0.5 M Ionic Strength and 25°C ^a

$^*\text{ML}_3^{2+}$	$^*E_{2,1}^{\circ},^b$ V	$^*E_{3,2}^{\circ},^b$ V	$10^{-9}k_q,$ $\text{M}^{-1} \text{s}^{-1}$
$\text{Ru}(5\text{-Clphen})_3^{2+}$	1.00	-0.77	1.32
$\text{Ru}(\text{bpy})_3^{2+}$	0.84	-0.84	0.63
$\text{Os}(5\text{-Clphen})_3^{2+}$	0.72	-0.85	0.55
$\text{Ru}(\text{phen})_3^{2+}$	0.79	-0.87	0.97
$\text{Ru}(5\text{-(CH}_3)\text{phen})_3^{2+}$	0.89	-0.90	1.15
$\text{Ru}(4,4'\text{-(CH}_3)_2\text{bpy})_3^{2+}$	0.69	-0.94	1.22
$\text{Os}(\text{phen})_3^{2+}$	0.57	-0.96	0.74
$\text{Ru}(4,7\text{-(CH}_3)_2\text{phen})_3^{2+}$	0.67	-1.01	1.63
$\text{Os}(5,6\text{-(CH}_3)_2\text{phen})_3^{2+}$	0.50	-1.03	1.48

^aConditions: 0.16 M Na_2SO_4 , pH 7.8, phosphate buffer. bpy: CoSO_4 is 5:1. ^bData taken from ref 6 and 7.

M CoSO_4 , 0.02 M bpy, 1.0 M TEOA·HCl, pH 8.1): 0%, 1; 30%, 5.6; 50%, 14. With 70% acetonitrile the mixture separated into two phases. Consequently 50% acetonitrile was used in subsequent experiments. Supplementary material Tables VI–VIII summarize preliminary results bearing on the dependence of H_2 production rate on TEOA, Co(II), and bpy concentrations and on pH for aqueous and 50% aqueous acetonitrile solutions. In Tables VII and VIII the dependence of the quantum yield for H_2 production on TEOA and $\text{Co}(\text{bpy})_3^{2+}$ concentration and pH in 50% aqueous acetonitrile are presented. The dependence of the H_2 quantum yield on the nature of the RuL_3^{2+} sensitizer ($(2\text{--}3) \times 10^{-4}$ M) in the presence of 5×10^{-3} M $\text{Co}(\text{bpy})_3^{2+}$ and 1.0 M tri-

Table V. Rate Constants k_q ($\times 10^9$, $\text{M}^{-1} \text{s}^{-1}$) for Quenching of $^*\text{Ru}(\text{bpy})_3^{2+}$ Emission as a Function of Supporting Electrolyte at 25°C and 0.5 M Ionic Strength^a

medium	quencher		
	$\text{Co}(\text{bpy})_3^{2+}$	$\text{Co}(\text{bpy})_3^{2+}$	$\text{Co}(\text{bpy})_3^{3+}$
NaF	0.043 (0.096 ^b)		
NaCl	0.047 (0.15 ^b)	1.01 ^c	2.95
NaBr	0.052 (0.18 ^b)	1.35	3.64
Na_2SO_4	0.042 (0.10 ^b)	0.68	2.08

^aSolutions contained 0.5 M NaX (0.17 M Na_2SO_4) and 0.025 M phosphate buffer at pH 6.0 for $\text{Co}(\text{bpy})_3^{2+}$ and pH 8.0 for $\text{Co}(\text{bpy})_3^{3+}$. ^bSensitizer is $\text{Ru}(4,7\text{-(CH}_3)_2\text{phen})_3^{2+}$. ^cMeasurements of the ionic strength dependence of k_q with NaCl supporting electrolyte yielded the following data [μ (M), $10^{-9}k_q$ ($\text{M}^{-1} \text{s}^{-1}$): 0.03, 0.28; 0.28, 0.64; 0.78; 1.0; 1.3; 1.5, 1.2].

Table VI. Rate Constants k ($\times 10^8$, $\text{M}^{-1} \text{s}^{-1}$) for the Reduction of RuL_3^{3+} by $\text{Co}(\text{bpy})_3^{2+}$

medium	L		
	phen	4,7-(CH_3) ₂ phen	3,4,7,8-(CH_3) ₄ phen
50% aq CH_3CN (0.25 M LiCl)	0.48	0.22	0.20
water (0.25 M LiCl)	1.9	3.1	
water (0.166 M Na_2SO_4)	2.5	5.1	

Table VII. Variation of H₂ Production Yields with Co(bpy)₃²⁺ and TEOA Concentrations (50% aq CH₃CN, μ = 0.25 M LiCl) at 25 °C^a

[TEOA], M	[Co(bpy) ₃ ²⁺], M	φ _{H₂}
0.10	0.04	0.0067
0.10	0.03	0.0086
0.10	0.02	0.021
0.25	0.03	0.036
0.25	0.01	0.092
0.50	0.03	0.080
0.50	0.01	0.17
0.50	0.0075	0.18
0.50	0.005	0.20

^a Irradiation of 2.5 × 10⁻⁴ M Ru(4,7-(CH₃)₂phen)₃²⁺ with visible light (λ ≥ 400 nm); pH 8.0 ± 0.1. Values have been corrected for the extent of quenching by the Co(bpy)₃²⁺ (K_{SV} = 1390 M⁻¹). H₂ evolution rates were 0.4–10 mL/h with 20 mL of solution. Typically a brief induction period due to residual O₂ in the solution was followed by production of H₂ at a constant rate; φ_{H₂} values tabulated are calculated from the slope of moles of H₂ vs. time plots for the latter region.

Table VIII. H₂ Yields as a Function of pH^a

pH	[TEOA]/[Co(II)] ^b	φ _{H₂} ^c
7.46	12	0.11
7.80	21	0.14
8.11	29	0.17
8.38	36	0.19
8.75	43	0.16

^a The solution contained 2.5 × 10⁻⁴ M Ru(4,7-(CH₃)₂phen)₃²⁺, 0.01 M Co(bpy)₃²⁺, and 0.5 M total TEOA adjusted to the pH given with HCl before addition of acetonitrile (final 50% aqueous acetonitrile). ^b The pK_a value 7.95 was used in calculating [TEOA]. ^c Corrected for *RuL₃²⁺ not quenched by Co(bpy)₃²⁺ (K_{SV} = 1390 M⁻¹).

Table IX. CoL₃^{3+/2+/+} Potentials (vs. NHE) Appropriate to Aqueous Solution ~25 °C

L	E _{3,2} ^o , V	E _{2,1} ^o , V	ΔE ^o , V	E _{3,1} ^o , V
bpy	0.30	-0.95	1.25	-0.33
(CH ₃) ₂ bpy	0.16	-1.07	1.25	-0.45
5-Clphen	0.50	-0.83	1.31	-0.18
phen	0.37	-0.93	1.30	-0.29
4,7-(CH ₃) ₂ phen	0.19	-1.07	1.26	-0.44
(H ₂ O) ₆	1.9	-1.44	3.34	+0.23

ethanolamine at pH 8.4 and 25 °C. The quantum yields determined are 0.12, 0.028, 0.23, and 0.23 for L = 5-Clphen, phen, 4,7-(CH₃)₂phen, and 3,4,7,8-(CH₃)₄phen, respectively.

Discussion

CoL₃ⁿ⁺ Reduction Potentials. It is interesting that CoL₃^{3+/2+} potentials vs. NHE in water (0.16 M Na₂SO₄) and vs. SCE in acetonitrile (0.1 M (R₄N)ClO₄) (Table I) are identical within experimental error (±0.01 V). As mentioned earlier, none of the CoL₃^{2+/+} couples studied was electrochemically well-behaved in aqueous media. To estimate the CoL₃^{2+/+} E^o values in water we use the acetonitrile E_{1/2} values corrected for liquid junction contributions as reflected in the E_{1/2} of the ferrocene-ferrocinium couple,¹³ i.e., E_{aq}^o (vs. NHE) = E_{AN}^o (vs. SCE) + 0.026 V. The Co(III)–Co(II) and Co(II)–Co(I) E^o values thus obtained are compiled in Table IX, where calculated Co(III)–Co(I) reduction potentials are also presented. The values are in good agreement with previously reported values in comparable media.¹⁴ For the polypyridine complexes, E_{3,2}^o ranges between +0.16 and +0.50 V, E_{2,1}^o between -0.83 and -1.07 V, and E_{3,1}^o between -0.18 and -0.45 V. In general the three potentials parallel each other with the difference between E_{3,2}^o and E_{2,1}^o being 1.25 ± 0.05 V

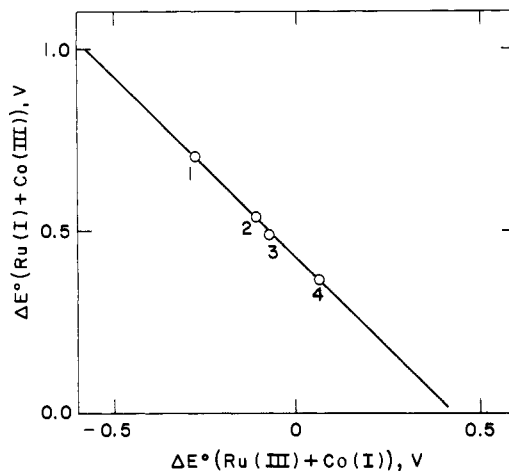
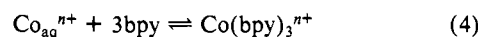


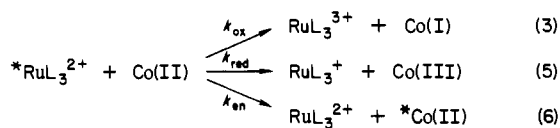
Figure 1. Plot of the driving force for reductive quenching (eq 5) vs. the driving force for oxidative quenching (eq 3) with RuL₃²⁺ as sensitizer and Co(bpy)₃²⁺ as quencher.

(for the ruthenium series, the corresponding potential difference is 2.52 ± 0.04 V, but the 2+/+ reduction process involves ligand rather than metal reduction⁷). As is usually found for 1,10-phenanthroline and 2,2'-bipyridine, the thermodynamic properties of the complexes strongly correlate with the basicities of the free ligands (and therefore with each other). It is noteworthy that in the CoL₃ⁿ⁺ series the polypyridines stabilize both Co(III) and Co(I) with respect to Co(II), with the relative stabilization of Co(III) being somewhat greater, e.g., for eq 4, K_{III} = 1.3 × 10²⁶ M⁻³, K_{II} = 6.6 × 10¹⁵ M⁻³, and K_I = 4.0 × 10²³ M⁻³.



The Co(III)–Co(I) potentials all lie below NHE but vary sufficiently that thermodynamic differences with respect to water reduction to H₂ by Co(I) might be expected.

Quenching Mechanisms. The CoL₃²⁺ complexes quench *RuL₃²⁺ emission with rate constants ranging from ~4 × 10⁷ to ~1 × 10⁹ M⁻¹ s⁻¹ for L = bpy at 0.5 M ionic strength and 25 °C. Three quenching mechanisms, excited-state oxidation, excited-state reduction, and energy transfer, must be considered, i.e.,



In differentiating between these pathways the redox properties (eq 3 or 5) and spectroscopic properties (eq 6) of sensitizer and quencher serve as a guide. For the CoL₃²⁺ complexes as quenchers (Tables III and IV), the CoL₃^{3+/2+/+} E^o data in Table IX and the RuL₃²⁺ and OsL₃²⁺ excited-state redox potentials (see Table IV) indicate that in all cases formation of Co(III) (eq 5) is thermodynamically favored, while formation of Co(I) (eq 3) is favorable in only some of the systems. Because of the CoL₃^{3+/2+} and CoL₃^{2+/+} (and *RuL₃²⁺/RuL₃⁺ and RuL₃³⁺/*RuL₃²⁺) E^o correlations mentioned earlier, as the one process becomes more favorable, the other becomes less favorable thermodynamically. This is illustrated in Figure 1, where the free-energy change for eq 5 is plotted against the free-energy change for eq 3 with Co(bpy)₃²⁺ as quencher.

These two redox processes may contribute to the net quenching in a rather complicated way because the self-exchange rates for the two cobalt couples CoL₃^{2+/+} (eq 3, k₁₁ > 1 × 10⁸ M⁻¹ s⁻¹^{9a}) and CoL₃^{3+/2+} (eq 5, k₁₁ = 10–10² M⁻¹ s⁻¹¹⁵) differ greatly. (In addition there could be substantial differences among the CoL₃^{3+/2+} exchange rates.) In fact for most of the sensitizer–

(13) Sahami, S.; Weaver, M. J. *Electroanal. Chem.* **1981**, *122*, 155.

(14) (a) Chen, Y. W.; Santhanam, K. S. V.; Bard, A. J. *J. Electrochem. Soc.* **1982**, *129*, 61. (b) Rao, J. M.; Hughes, M. C.; Macero, D. J. *Inorg. Chim. Acta* **1979**, *35*, L369. (c) Margel, S.; Smith, W.; Anson, F. C. *J. Electrochem. Soc.* **1978**, *125*, 241. (d) Prasad, R.; Sciafe, D. B. *J. Electroanal. Chem. Interfacial Electrochem.* **1977**, *84*, 873.

(15) Neumann, H. M., quoted in: Farina, R.; Wilkins, R. G. *Inorg. Chem.* **1968**, *7*, 516.

Scheme I

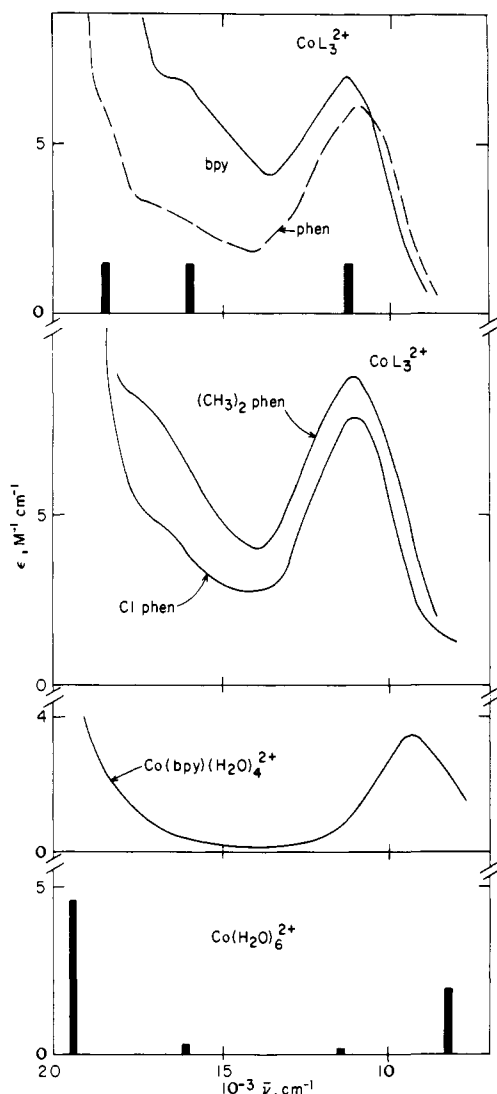
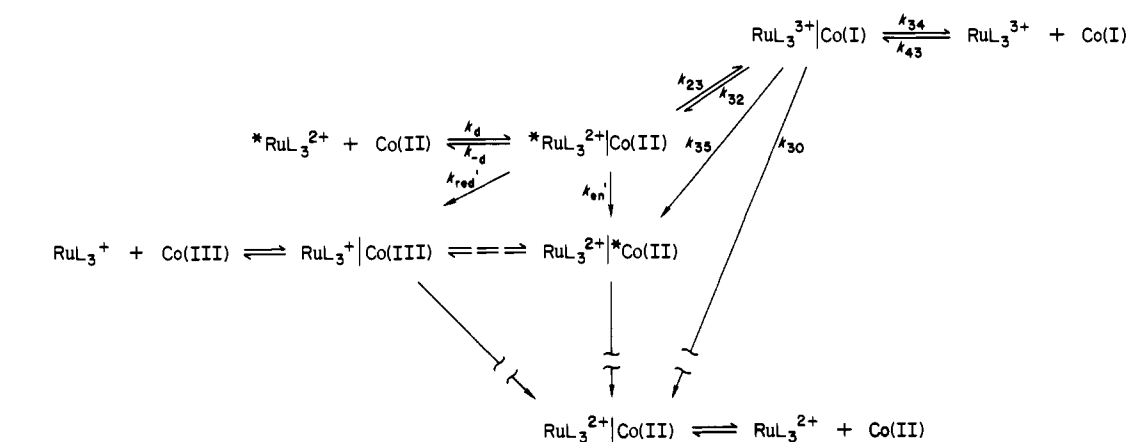


Figure 2. Near-IR-vis spectra of cobalt(II) complexes in water at 25 °C determined in this work. Top two frames: CoL_3^{2+} with $L = \text{bpy}$, phen , $4,7\text{-(CH}_3)_2\text{phen}$, and 5-Clphen . The bars in the top frame summarize the assignments for Co(bpy)_3^{2+} (ground state $^4\text{T}_{1g}$) given by Palmer and Piper:^{16a} $1.13 \mu\text{m}^{-1}$, $^4\text{T}_2(\text{F})$; $1.60 \mu\text{m}^{-1}$, $^2\text{T}_1$, $^2\text{T}_1(\text{G})$; $1.85 \mu\text{m}^{-1}$, $^2\text{T}_1(\text{P,H})$; (not shown) $2.20 \mu\text{m}^{-1}$, $^4\text{T}_1(\text{P})$ (the heights have no significance). In the bottom frame the bars (heights are ϵ_{max}) are assignments given by Jørgensen^{16b} for $\text{Co(H}_2\text{O)}_6^{2+}$ (ground state $^4\text{T}_{1g}$): $0.81 \mu\text{m}^{-1}$, $^4\text{T}_{2g}$; $1.13 \mu\text{m}^{-1}$, ^2T ; $1.60 \mu\text{m}^{-1}$, $^4\text{A}_{2g}$; $1.94 \mu\text{m}^{-1}$, $^4\text{T}_{1g}(\text{P})$.

quencher pairs, oxidative quenching is favored kinetically (though not thermodynamically) because the intrinsic electron-transfer barrier for the $\text{CoL}_3^{2+/+}$ couple is so small. In addition, energy-transfer paths cannot be neglected in these systems. The

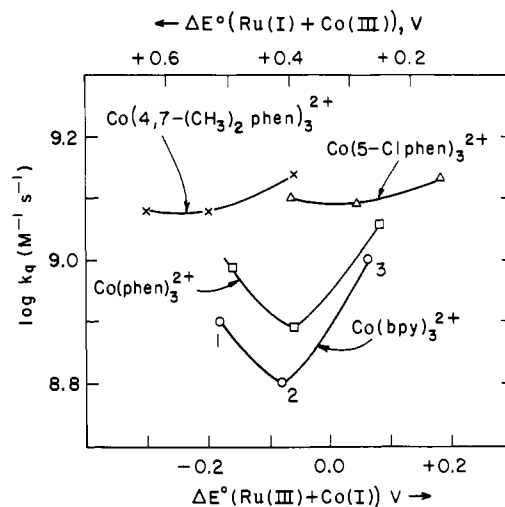


Figure 3. Rate constants (Table III) for the quenching of (polypyridine)ruthenium(II) emission by CoL_3^{2+} as a function of (bottom axis) the driving force for oxidative quenching [top axis: driving force for reductive quenching is exact for Co(bpy)_3^{2+} but only approximate for the other Co(II) complexes].

RuL_3^{2+} ($1.5\text{--}1.7 \mu\text{m}^{-16}$) and OsL_3^{2+} ($1.3\text{--}1.5 \mu\text{m}^{-17}$) emission bands overlap the CoL_3^{2+} absorption bands¹⁶ (see Figure 2). Confirmation of the anticipated complexity of the quenching mechanism(s) is presented in Figure 3, where the logarithms of the k_q values in Table III are plotted as a function of the driving force for oxidative (bottom axis) or reductive (top axis) electron-transfer quenching. The quenchers Co(bpy)_3^{2+} and Co(phen)_3^{2+} behave similarly, and for them k_q is a minimum with Ru(phen)_3^{2+} . By contrast, $\text{Co(5-Clphen)}_3^{2+}$ and $\text{Co(4,7-(CH}_3)_2\text{phen)}_3^{2+}$ quench much more rapidly, with k_q values that are essentially independent of sensitizer.

Scheme I includes the parallel quenching processes, eq 3, 5, and 6. The vertical ordering of the various species in the scheme illustrates approximately their relative energies in the $\text{Ru(bpy)}_3^{2+}\text{--Co(bpy)}_3^{2+}$ system. The energy of the excited cobalt(II) species is the least certain and is discussed further below. The following expression for k_q is derived for Scheme I when the steady-state approximation is applied to the concentrations of the various intermediates:

$$k_q = k_{\text{red}} + k_{\text{ox}} + k_{\text{en}} \quad (7a)$$

where

$$k_{\text{red}} = \frac{k_d k_{\text{red}}' (k_{30}' + k_{32} + k_{34})}{\text{DEN}} \quad (7b)$$

(16) (a) Palmer, R. A.; Piper, T. S. *Inorg. Chem.* **1966**, *5*, 864. (b) Jørgensen, C. K. *Adv. Chem. Phys.* **1963**, *5*, 3. Lever, A. B. P. "Inorganic Electronic Spectroscopy"; Elsevier: New York, 1968; p 317.

$$k_{\text{ox}} = \frac{k_d k_{23} (k_{30}' + k_{34})}{\text{DEN}} \quad (7c)$$

$$k_{\text{en}} = \frac{k_d k_{\text{en}}' (k_{30}' + k_{32} + k_{34})}{\text{DEN}} \quad (7d)$$

$$\text{DEN} = (k_{-d} + k_{23} + k_{\text{red}}' + k_{\text{en}}') (k_{30}' + k_{34}) + k_{32} (k_{-d} + k_{\text{red}}' + k_{\text{en}}')$$

and $k_{30}' = k_{30} + k_{35}$. Note that Scheme I is oversimplified in showing the decay of $\text{RuL}_3^{2+} \text{Co(II)}$ producing only $\text{RuL}_3^{2+} \text{Co(II)}$. Of course, if Co(II) is sufficiently long-lived, $\text{RuL}_3^{2+} \text{Co(II)}$ could dissociate prior to the decay of the Co(II) .

Quenching by Co(bpy)_3^{2+} . The values of k_{red} , k_{ox} , k_{en} , and k_q calculated¹⁷ from the above equations for Co(bpy)_3^{2+} quenching of RuL_3^{2+} are plotted vs. the driving force for oxidative quenching in Figure 4. The parameters used in constructing these curves are given in the figure caption and the points are the Co(bpy)_3^{2+} quenching rate constants (at $\mu = 0.5$ M) from Table IV. The calculated composite (solid) curve gives a satisfactory fit to the RuL_3^{2+} data although the observed k_q values for the phen derivatives are somewhat higher than both the calculated curve and the values for the bpy derivatives. The measured values for the OsL_3^{2+} quenching reactions fall below the calculated composite curve. A somewhat smaller value for k_{en}' (1.0×10^9 s⁻¹ compared to 1.2×10^9 s⁻¹ used for RuL_3^{2+}) appears appropriate. It is evident that k_{red} contributes <10% to the net value of k_q in the RuL_3^{2+} quenching. Because OsL_3^{2+} is a poorer oxidant (Table IV) the contribution of k_{red} for OsL_3^{2+} (not shown) is even smaller.

The plots in Figure 4 manifest several interesting features. First, although the intrinsic rate constant for energy transfer from RuL_3^{2+} (k_{en}) was assumed to be independent of ΔE° , the contribution of k_{en} to k_q does depend on ΔE° through the driving-force dependence of the competing redox pathways k_{23} and k_{red} , with the oxidative pathway approaching the diffusion-controlled limit (k_d) when ΔE for the formation of RuL_3^{3+} and Co(bpy)_3^+ becomes sufficiently large. Second, the absence of (reflection) symmetry between the k_{ox} and k_{red} curves derives from the different exchange rate constants and nonadiabaticities (κ values) for the two pathways. As noted above, the exchange rate of the $\text{Co(III)}\text{--Co(II)}$ couple is ~ 7 orders of magnitude smaller than that of the $\text{Co(II)}\text{--Co(I)}$ couple, and the electron-transfer reactions of the former couple are much less adiabatic than are those of the latter. The small $\text{Co(III)}\text{--Co(II)}$ exchange rate causes the reductive quenching rates to approach saturation much more slowly than the oxidative quenching rates, while the poor electronic factors for the production of $\text{CoL}_3^{3+} + \text{RuL}_3^+$ cause the reductive quenching rates to saturate below the diffusion-controlled limit. This will be discussed further in a future publication.^{18a} In summary, it is evident from the calculated curve in Figure 4 that eq 3 and 6 are sufficient to account for the trends in the measured k_q values, with energy-transfer quenching (eq 6) predominating for the majority of the RuL_3^{2+} systems but with oxidative quenching the dominant quenching mode for reaction partners such as $\text{Ru(4,7-(CH}_3)_2\text{phen)}_3^{2+}$ and Co(bpy)_3^{2+} . This is cor-

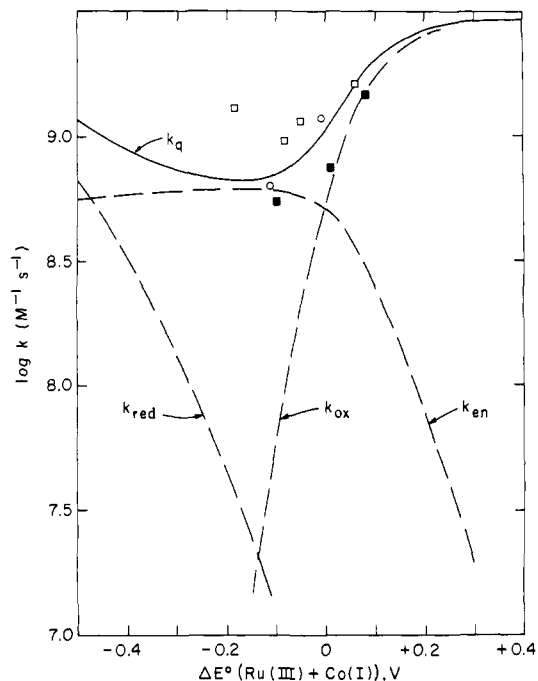


Figure 4. Values of k_{red} , k_{ox} , k_{en} , and k_q for quenching of RuL_3^{2+} emission by Co(bpy)_3^{2+} at 0.5 M ionic strength (Na_2SO_4), calculated from eq 7 as a function of the driving force for the oxidative pathway. The curves were calculated by using $k_d = 3 \times 10^9$ M⁻¹ s⁻¹, $k_{-d} = 4.5 \times 10^9$ s⁻¹, $k_{30}' + k_{34} = 2.4 \times 10^{10}$ s⁻¹, $k_{\text{en}}' = 1.2 \times 10^9$ s⁻¹, and the following literature values of k (0.1 M ionic strength) and κ for the couples: $\text{RuL}_3^{3+}/\text{RuL}_3^{2+}$, 6×10^8 M⁻¹ s⁻¹, 1; $\text{Co(bpy)}_3^{2+}/\text{Co(bpy)}_3^+$, 6×10^8 M⁻¹ s⁻¹, 1; $\text{RuL}_3^{2+}/\text{RuL}_3^+$, 1×10^8 M⁻¹ s⁻¹, 1; $\text{Co(bpy)}_3^{3+}/\text{Co(bpy)}_3^{2+}$, 18 M⁻¹ s⁻¹, 10^{-3} . The values of κ for the oxidative and reductive quenching paths were 1 and 10^{-3} , respectively, and A was 6×10^{12} M⁻¹ s⁻¹.¹⁷ The experimental points are from Table IV: (■) OsL_3^{2+} ; (□) RuL_3^{2+} (phen derivatives); (○) RuL_3^{2+} (bpy derivatives).

roborated for the $\text{Co(bpy)}_3^{2+}\text{--Ru(4,7-(CH}_3)_2\text{phen)}_3^{2+}$ system by the observation that Ru(III) and Co(I) are produced in flash-photolysis experiments (vide infra). Remarkably k_{red} contributes negligibly to k_q despite the favorable thermodynamics. As mentioned above, the reduction of CoL_3^{2+} to CoL_3^+ is kinetically favored even when the free-energy change is very small because of the high self-exchange rate of the $\text{Co(II)}\text{--Co(I)}$ couple; by contrast, oxidation of CoL_3^{2+} to CoL_3^{3+} attains a comparable rate only at a driving force of >0.5 eV because of the much smaller exchange rate of the $\text{CoL}_3^{3+}/2+$ couple and because of the poor electronic factor for the reaction.

The possibility that the products of the energy-transfer path (electronically excited quencher) can also be produced through the electron-transfer quenching paths (and vice versa) also needs to be considered, and such pathways are included in Scheme I. For concreteness, we consider that the Co(II) in Scheme I is the $[(t_{2g})^6(e_g)^1]^2\text{T}$ state of Co(bpy)_3^{2+} which is formed in the transition at $1.6 \mu\text{m}^{-1}$ (Figure 2). The thermally equilibrated ^2T state can be estimated to lie ~ 0.5 eV below the Franck-Condon state,^{18b,19a} and the equilibrated ^2T state therefore lies ~ 1.6 eV above the ground state. Consequently the formation of $\text{RuL}_3^{2+} \text{Co(bpy)}_3^{2+}$ from $\text{RuL}_3^{3+} [\text{Co(bpy)}_3^+]$ would be favorable by ~ 0.5 eV, while its formation from $\text{RuL}_3^+ [\text{Co(bpy)}_3^{3+}]$ would be favorable by ~ 0.1 eV. Because of its small driving force, the conversion of $\text{RuL}_3^+ [\text{Co(bpy)}_3^{3+}]$ to $\text{RuL}_3^{2+} [\text{Co(bpy)}_3^{2+}]$ is unlikely to compete with the direct formation of the corresponding ground-state products (unless the latter reaction is in the inverted region). Similarly, the conversion of $\text{RuL}_3^{2+} [\text{Co(bpy)}_3^{2+}]$ to $\text{RuL}_3^+ [\text{Co(bpy)}_3^{3+}]$ can be neglected because of the short lifetime of Co(bpy)_3^{2+} (probably less than 1 ns), the small driving force for the

(17) Electron-transfer rate constants k_{ij} were calculated from

$$k_{ij} = \kappa_{ij} (k_{ii} K_{ij} f_{ij} / \kappa_{ii} \kappa_{jj})^{1/2} W_{ij}$$

$$\ln f_{ij} = \frac{[\ln K_{ij} + (w_{ij} - w_{ji}) / RT]^2}{4 \left[\ln \left(\frac{k_{ii} k_{jj}}{\kappa_{ii} \kappa_{jj} A_{ii} A_{jj}} \right) + \frac{w_{ii} + w_{jj}}{RT} \right]}$$

$$W_{ij} = \exp[-(w_{ij} + w_{ji} - w_{ii} - w_{jj}) / 2RT]$$

where k_{ii} and k_{jj} are self-exchange rates for the relevant cobalt and ruthenium couples, K_{ij} is the equilibrium constant for the electron-transfer process, the w terms are work corrections, and the A terms are preexponential factors in the rate constant expressions.

(18) (a) Brunschwig, B. S.; Sutin, N., work in progress. (b) Szalda, D. J.; Macartney, D. H.; Sutin, N. *Inorg. Chem.* **1984**, *23*, 3473. (c) Liu, D. K.; Sutin, N., work in progress.

(19) For recent treatments of energy-transfer processes involving metal complexes, see: (a) Creutz, C.; Chou, M.; Netzel, T. L.; Okumura, M.; Sutin, N. *J. Am. Chem. Soc.* **1980**, *102*, 1309. (b) Balzani, V.; Bolletta, F.; Scandola, F. *J. Am. Chem. Soc.* **1980**, *102*, 2152.

electron transfer, and the relatively large intrinsic barrier for the $^*Co(bpy)_3^{2+}-Co(bpy)_3^{3+}$ exchange. (By analogy with the $Ni(bpy)_3^{2+}-Ni(bpy)_3^{3+}$ exchange^{18a} the rate constants for the $^*Co(bpy)_3^{2+}-Co(bpy)_3^{3+}$ and $Co(bpy)_3^{3+}-^*Co(bpy)_3^{2+}$ exchanges are expected to be $\sim 10^3 M^{-1} s^{-1}$ since all three exchanges involve the transfer of an e_g electron.) By contrast, the formation of $RuL_3^{2+}|^*Co(bpy)_3^{2+}$ from $RuL_3^{3+}|Co(bpy)_3^{3+}$ is more exergonic and it is possible that this reaction (k_{35}) can compete with the cage escape (k_{34}), with the formation of $^*RuL_3^{2+}|Co(II)$ (k_{32}), and also with direct formation of ground-state products $RuL_3^{2+}|Co(II)$ (k_{30}) since the latter reaction lies in the inverted region.^{18c} Note that in the analysis of the kinetic data in Figure 4 the value of $k_{30}' + k_{34}$ has been assumed to be equal to $2.4 \times 10^{10} s^{-1}$, independent of the driving force. The latter assumption can, of course, be relaxed if warranted. Not considered in Scheme I is the formation of electronically excited redox products ($^*Co(III)$ or $^*Co(I)$, etc.) in the electron-transfer quenching paths; their formation is not thermodynamically favorable in the present system. The formation of excited species as primary products of the redox quenching paths is considered elsewhere.^{18a}

Quenching by CoL_3^{2+} Complexes. Scheme I and eq 7 are also applicable to quenching by other CoL_3^{2+} complexes (Figure 3 and Table III). However, since the bpy and phen systems are very similar and exchange rate data are not available for the substituted phen $CoL_3^{3+/2+}$ couples, we confine our modeling to that present in Figure 4. As noted earlier, $Co(phen)_3^{2+}$ and $Co(bpy)_3^{2+}$ exhibit very similar sensitizer dependences (Figure 3). Thus the $Co(phen)_3^{2+}$ quenching appears to proceed by parallel energy transfer ($k_{en} \approx 0.5 \times 10^9 M^{-1} s^{-1}$ at 0.1 M ionic strength) and oxidative quenching paths as shown for $Co(bpy)_3^{2+}$ in Figure 4. The larger, sensitizer-independent (when ΔE_{ox} is unfavorable) k_q values for the substituted phen derivatives indicate that energy-transfer paths predominate for these CoL_3^{2+} quenchers ($k_{en} \approx 1.3 \times 10^9 M^{-1} s^{-1}$ at 0.1 M ionic strength).

Consider the CoL_3^{2+} series (Table II)—the $Co(bpy)_3^{2+/+}$ potential is $-1.23 V^{9b}$ and the $Co(bpy)_3^{3+/2+}$ potential is $+0.84 V^{20}$. The absorption spectrum of $Co(bpy)_3^{2+}$ (Figure 2) substantially overlaps the emission spectra of the RuL_3^{2+} complexes. Rate constants for quenching by CoL_3^{2+} range from $5.5 \times 10^7 M^{-1} s^{-1}$ with $^*Ru(bpy)_3$ ($E_{2,1}^\circ = +0.84 V$, $E_{3,2}^\circ = -0.84 V$) to $\sim 3 \times 10^7 M^{-1} s^{-1}$ for the phen derivatives ($E_{2,1}^\circ = +0.67$ to $+1.0 V$, $E_{3,2}^\circ = -0.77$ to $-1.01 V$).^{6,7} From these E° and other data, outer-sphere electron-transfer rate constants for eq 3 and 5 are estimated¹⁷ as $k_{red} \leq 1 \times 10^5 M^{-1} s^{-1}$ and $k_{ox} = 1 \times 10^4$ to $2 \times 10^7 M^{-1} s^{-1}$ (the latter value is for $^*Ru(4,7-(CH_3)_2phen)_3^{2+}$). Thus only for the $Co(bpy)_3^{2+}$ quenching of $^*Ru(4,7-(CH_3)_2phen)_3^{2+}$ is the estimated electron-transfer rate sufficiently large to contribute significantly to the observed quenching rate constant. This, taken with the fact that k_q values for all four sensitizers are extremely similar, suggests that energy transfer is the predominant process in $Co(bpy)_3^{2+}$ quenching. Since E° data are not available for the other CoL_3^{2+} quenchers, electron-transfer rates cannot be estimated for the other entries in Table II. However, in view of the relative insensitivity of k_q to both quencher and sensitizer it is likely that energy transfer predominates for these as well. The small increase in k_q from $Ru(5-Clphen)_3^{2+}$ to $Ru(4,7-(CH_3)_2phen)_3^{2+}$ for several of the CoL_3^{2+} quenchers suggests that oxidative quenching, eq 3, may contribute to k_q with $Ru(4,7-(CH_3)_2phen)_3^{2+}$.

Energy Transfer. Energy-transfer paths appear quite prevalent with cobalt(II) complexes as quenchers (and Co(III); see ref 12). Because of the wealth of ligand-field transitions between 0.8 and $1.6 \mu m^{-1}$ in the spectra of Co(II) complexes (Figure 2, ref 16), it is evident that there are low-energy cobalt(II)-acceptor states. Thus energy transfer from the ruthenium(II) and osmium(II) excited states (excitation energies E typically 1.60 and $1.40 \mu m^{-1}$, respectively) to cobalt(II) complexes are generally thermodynamically favorable.¹⁹ In fact, as shown in Figure 2 the Co(II) spectra do not vary greatly from one (six-coordinate) complex to another. The lowest energy band (a quartet-quartet transition) shifts $0.34 \mu m^{-1}$ (from 0.79 to $1.13 \mu m^{-1}$) on going from Co-

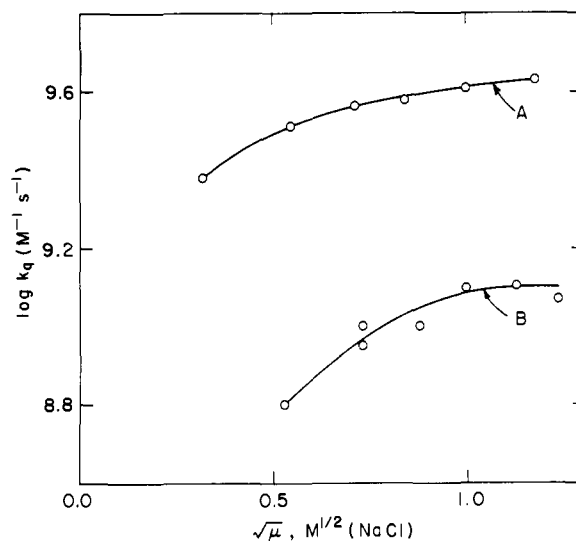


Figure 5. Quenching rate constants as a function of ionic strength at 25 °C. (A) $S = Ru(4,4'-(CH_3)_2bpy)_3^{2+}$, $Q =$ diquat. (B) $S = ^*Ru(bpy)_3^{2+}$, $Q = Co(bpy)_3^{2+}$.

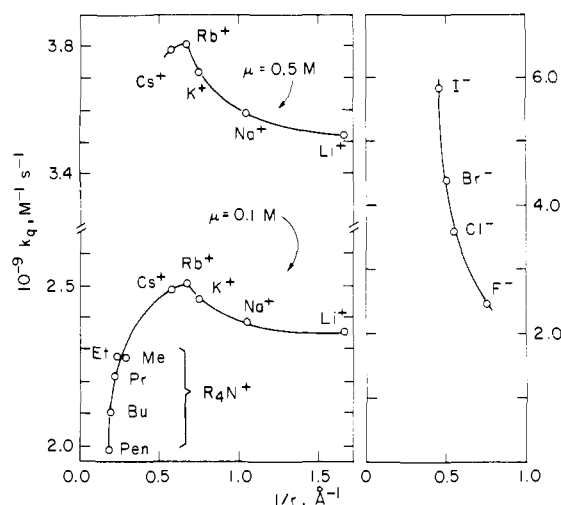


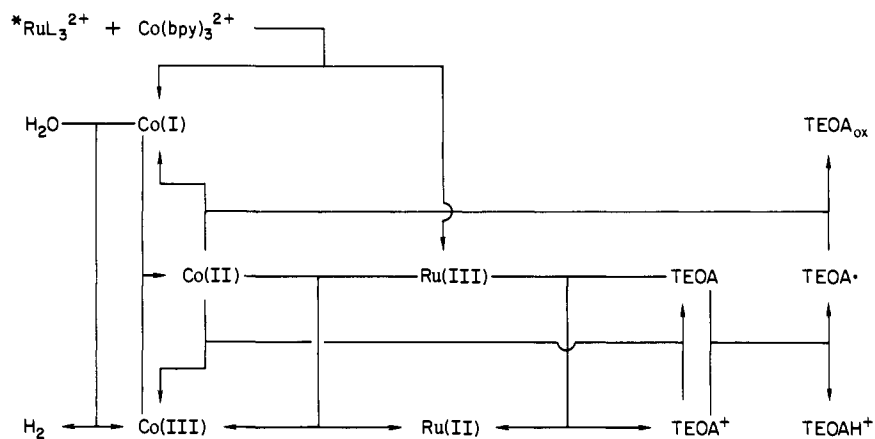
Figure 6. Dependence of quenching rate constants on the ionic radius of the supporting electrolyte cation (chloride salt) and anion (sodium salt) at 25 °C and 0.5 M ionic strength ($S = Ru(bpy)_3^{2+}$, $Q =$ diquat). Abbreviations for the tetraalkylammonium cations: Me = CH_3 , Pr = C_3H_7 , Bu = C_4H_9 , Pen = C_5H_{11} .

$(H_2O)_6^{2+}$ to $Co(bpy)_3^{2+}$; the position of the next lowest band (a quartet-doublet transition) differs by $0.49 \mu m^{-1}$ ($1.11 \mu m^{-1}$ vs. $1.6 \mu m^{-1}$) for these two complexes. Interestingly, the rate constants for energy transfer from $^*Ru(phen)_3^{2+}$ to these two complexes differ by nearly 10^4 ($2 \times 10^5 M^{-1} s^{-1}$ for $Co(H_2O)_6^{2+}$ vs. $0.8 \times 10^9 M^{-1} s^{-1}$ for $Co(bpy)_3^{2+}$). The corresponding rate constant with $Co(bpy)(H_2O)_4^{2+}$ (whose absorption spectrum resembles that of $Co(H_2O)_6^{2+}$ —but is shifted $0.1-0.2 \mu m^{-1}$ to higher energy) is intermediate, $5 \times 10^7 M^{-1} s^{-1}$. In view of the similarities in the $^*RuL_3^{2+}-Co(II)$ spectral overlap with these three cobalt(II) complexes, it is tempting to speculate that the observed rate range derives from changing electronic factors for the energy-transfer process, with k_{en} (the probability of energy transfer) being greatest for $Co(bpy)_3^{2+}$ ($\geq 10^{-4}$) and smallest for $Co(H_2O)_6^{2+}$ ($\geq 10^{-8}$). Electronic coupling for the $^*RuL_3^{2+}-Co(bpy)_3^{2+}$ reactant pair could be favored by several factors—among them, stacked bpy-L interactions coupling the bpy-L (and thereby the Ru and Co) orbitals, as well as the energetic proximity of redox states ($Co(I)-Ru(III)$ and $Co(III)-RuL_3^{2+}$) which could couple the reactant and product states. It is interesting that the energy-transfer rate constants for CoL_3^{2+} appear to be a function of L despite the fact

(20) Farina, R.; Wilkins, R. G. *Inorg. Chem.* 1968, 7, 516.

(21) Demas, J. N.; Addington, J. W.; Peterson, S. H.; Harris, E. W. J. *Phys. Chem.* 1977, 81, 1039.

Scheme II



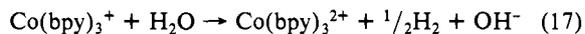
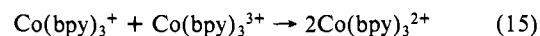
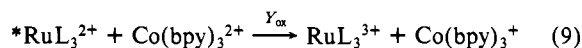
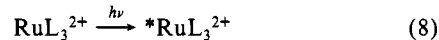
that the absorption spectra change little with L (see Figure 2). This too might result from subtle changes in the electronic factors for the energy-transfer process.

Medium Effects. The ionic strength dependences of the $\text{Co}(\text{bpy})_3^{2+}$ and diquat quenching rate constants (data from Table V and ref 22, respectively) are plotted in Figure 5, and the cation dependence of the diquat quenching rate constant is shown in Figure 6. Although the effect of ionic strength on quenching rate constants can be discussed in terms of the Brønsted-Debye equations, the data were not fit to such expressions because the kinetics exhibit specific ion effects. The rate constants do increase with increasing ionic strength as is expected for a process involving the diffusion together of two similarly charged species. The striking specific ion effects in Figure 6 parallel the behavior observed in the enthalpies of transfer of ions from H_2O to D_2O ²³ and also in the variation of Walden products of ions²⁴ as a function of the reciprocal of the ionic radius. These effects have been attributed to ion-solvent interactions that are unique for water. The structure-promoting cations and anions (whether it is through specific ion-dipole hydration or through hydrophobic interactions) decrease the quenching rate constants, whereas the structure-breaking cations and anions enhance the quenching rate constants. The cation effects observed in this work are similar (but much smaller in magnitude) to those seen in reactions between negatively charged complexes, for example, $\text{Fe}(\text{CN})_6^{4-}$ and IrCl_6^{2-} .²⁵ While these empirical correlations can be identified, it is not feasible to model them in any depth because, in terms of a detailed model such as Scheme I, the specific ion effects may originate from changes in k_d and k_{-d} (through the work term¹⁷), or k_{23} and k_{32} (through the driving force for electron transfer, or the electronic factor, or the outer-shell barrier¹⁷).

Water Photoreduction. Water photoreduction systems based on both oxidative²⁶ and reductive quenching^{2,3,27} of the (polypyridine)ruthenium(II) excited states have been developed. In the $\text{TEOA}-\text{Co}(\text{bpy})_n^{2+}-\text{Ru}(4,7-(\text{CH}_3)_2\text{phen})_3^{2+}$ 50% aqueous CH_3CN system, although parallel quenching processes operate (see above), it is the oxidative process that is responsible for H_2 formation: in flash-photolysis experiments in 50% aqueous CH_3CN (0.25 M LiCl, 0.02 M TEOA, pH 8) excited-state quenching ($k_{\text{obsd}} = 7.5 \times 10^6 \text{ s}^{-1}$ with 0.01 M $\text{Co}(\text{bpy})_3^{2+}$ and 2.9

$\times 10^6 \text{ s}^{-1}$ with 0.003 M $\text{Co}(\text{bpy})_3^{2+}$; $k_q = 0.7 \times 10^9 \text{ M}^{-1} \text{ s}^{-1}$) leads to $\text{Ru}(4,7-(\text{CH}_3)_2\text{phen})_3^{3+}$ (440 nm, $\Delta\epsilon = 2.3 \times 10^4 \text{ M}^{-1} \text{ cm}^{-1}$) and $\text{Co}(\text{bpy})_3^+$ (605 nm, $\epsilon = 6.2 \times 10^3 \text{ M}^{-1} \text{ cm}^{-1}$)^{9a}) in 0.27 \pm 0.03 yield. At such low TEOA concentrations reduction of Ru(III) to Ru(II) occurs with a pseudo-first-order Co(II)-dependent rate constant, and the Co(I) produced decays on a much longer time scale ($>10 \mu\text{s}$) by second-order kinetics. Under optimal H_2 formation conditions, i.e., $[\text{TEOA}] \sim 1 \text{ M}$, Ru(III) is not detected as an intermediate but Co(I) is found as before.

The above observations suggest the following sequence²⁸ (L = 4,7-(CH_3)₂phen), which is also outlined in Scheme II:



The conventional back-reaction (10), although expected to be rapid ($k_{10} \geq 10^9 \text{ M}^{-1} \text{ s}^{-1}$), is not observed because of eq 11 for which $k_{11} = 5.1 \times 10^8 \text{ M}^{-1} \text{ s}^{-1}$ in water (0.16 M Na_2SO_4 , $\mu = 0.5 \text{ M}$) and $2.2 \times 10^7 \text{ M}^{-1} \text{ s}^{-1}$ in 50% aqueous CH_3CN (0.25 M LiCl, $\mu = 0.25 \text{ M}$). The rate of eq 11 is always great because of the high Co(II) levels required for excited-state quenching (eq 9). At sufficiently high $[\text{TEOA}]/[\text{Co}(\text{bpy})_3^{2+}]$, reduction of RuL_3^{3+} by TEOA (eq 12) becomes competitive.²³ Step 14, TEOA-catalyzed rearrangement of the primary (oxidizing) $\text{TEOA}^{\cdot+}$ radical to a reducing species TEOA^{\cdot} , step 16, reduction of $\text{Co}(\text{bpy})_3^{2+}$ by TEOA^{\cdot} , and step 17, reduction of water by $\text{Co}(\text{bpy})_3^+$, are written by analogy with previous results.^{3,26a} Step 13, oxidation of $\text{Co}(\text{bpy})_3^+$ by $\text{TEOA}^{\cdot+}$, is required by the data in Table VI (see below). In the absence of (or at low concentrations of) TEOA, $\text{Co}(\text{bpy})_3^+$ is oxidized by $\text{Co}(\text{bpy})_3^{3+}$ ($k_{13} \sim 1 \times 10^9 \text{ M}^{-1} \text{ s}^{-1}$), and no H_2 is produced.

The competition between RuL_3^{3+} oxidation of $\text{Co}(\text{bpy})_3^{2+}$ (eq 11) and of TEOA (eq 12) is evident in the data in Table VI and

(28) As noted earlier, even at $\geq 1 \text{ M}$ TEOA no quenching of ${}^*\text{RuL}_3^{2+}$ (L = bpy or 4,7-(CH_3)₂phen) occurs. The small quenching rate constant implicated, $<10^5 \text{ M}^{-1} \text{ s}^{-1}$, is consistent with other observations: the rate constant for reduction of $\text{Os}(\text{bpy})_3^{3+}$ (similar $E_{3,2}^{\circ}$ to ${}^*\text{RuL}_3^{2+}$) is $3.1 \times 10^3 \text{ M}^{-1} \text{ s}^{-1}$ in water (0.5 M NaCl) and $1.8 \times 10^4 \text{ M}^{-1} \text{ s}^{-1}$ in 50% aqueous CH_3CN (0.5 M tetrabutylammonium chloride) at 25 °C.

(22) Krishnan, C. V.; Creutz, C.; Schwarz, H. A.; Sutin, N. *J. Am. Chem. Soc.* **1983**, *105*, 5617.

(23) Friedman, H. L.; Kirshnan, C. V. "Water, A Comprehensive Treatise"; Franks, F., Ed.; Plenum Press: New York, 1973; Vol. 3, Chapter 1.

(24) Kay, R. L. "Water, A Comprehensive Treatise"; Franks, F., Ed.; Plenum Press: New York, 1973; Vol. 3, Chapter 4.

(25) Bruhn, H.; Nigam, S.; Holzwarth, J. F. *Discuss. Faraday Soc.* **1982**, *74*, 129.

(26) (a) Chan, S.-F.; Chou, M.; Creutz, C.; Matsubara, T.; Sutin, N. *J. Am. Chem. Soc.* **1981**, *103*, 369. (b) Keller, P.; Moradpour, E.; Amouyal, E.; Kagan, H. B. *Nouv. J. Chim.* **1980**, *4*, 377. (c) Borgarello, E.; Kiwi, J.; Pelizzetti, E.; Visca, M.; Grätzel, M. *J. Am. Chem. Soc.* **1981**, *103*, 6324 and references therein. (d) Lay, P. A.; Mau, A. W. H.; Sasse, W. H. F.; Creaser, I. I.; Gahan, L. R.; Sargeson, A. M. *Inorg. Chem.* **1983**, *22*, 2347.

(27) Brown, G. M.; Brunschwig, B. S.; Creutz, C.; Endicott, J. F.; Sutin, N. *J. Am. Chem. Soc.* **1979**, *101*, 1298.

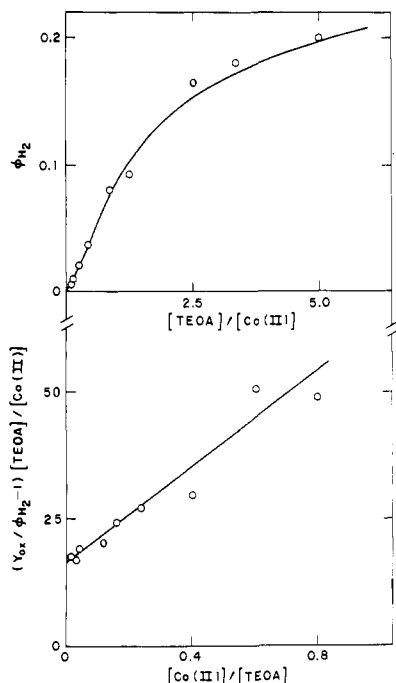


Figure 7. Dependence of quantum yields for H_2 formation on the ratio of triethanolamine and $Co(bpy)_3^{2+}$ concentrations (25 °C, 50% aqueous acetonitrile, 0.25 M ionic strength, $S = Ru(4,7-(CH_3)_2phen)_3^{2+}$; see Table VII). Bottom plot is suggested by eq 18 (see text).

in the plot at the top of Figure 7. In terms of eq 8–17 the quantum yield of H_2 (after correcting for the fraction of $*RuL_3^{2+}$ not quenched) is one-half the net $Co(bpy)_3^{3+}$ yield. Cobalt(I) is produced in eq 9 and 16 but oxidized by $Co(bpy)_3^{3+}$ in eq 15. Cobalt(III) is produced by both $Ru(bpy)_3^{3+}$ (eq 11) and $TEOA^+$ (eq 13) oxidants and the fates of both $Ru(bpy)_3^{3+}$ and $TEOA^+$ are $[TEOA]$ dependent (eq 12 and 14). Provided that eq 15 and 16 are rapid and that eq 10 can be neglected, the H_2 yield is determined by Y_{ox} and the efficiency of conversion of $Ru(bpy)_3^{3+}$ to $TEOA^+$. Scheme II (eq 8–17) gives the following expression for the H_2 yield when the steady-state approximation is applied to the concentrations of the various intermediates.

$$\phi_{H_2} = Y_{ox} \left\{ \frac{k_{12}[TEOA]}{k_{11}[Co(bpy)_3^{2+}] + k_{12}[TEOA]} \right\} \times \left\{ \frac{k_{14}[TEOA]}{k_{13}[Co(bpy)_3^{2+}] + k_{14}[TEOA]} \right\} \quad (18)$$

Equation 18 suggests the plot of $[(Y_{ox}/\phi_{H_2}) - 1][TEOA]/[Co(bpy)_3^{2+}]$ vs. $[Co(bpy)_3^{2+}]/[TEOA]$ shown at the bottom of Figure 7. The value $Y_{ox} = 0.27$ (from the flash-photolysis measurements) was used in constructing the plot. From the magnitudes of the intercept ($=k_{11}/k_{12} + k_{13}/k_{14}$) and slope ($=k_{11}k_{13}/k_{12}k_{14}$), the rate constant ratios k_{11}/k_{12} or k_{13}/k_{14} are 12.8 ± 0.5 and 3.8 ± 0.5 . From flash-photolysis measurements $k_{11} = 2.2 \times 10^7 M^{-1} s^{-1}$ and $k_{12} = 5.2 \times 10^6 M^{-1} s^{-1}$ in this medium, giving $k_{11}/k_{12} = 4.2$, in reasonable agreement with the ratio 3.8 ± 0.5 obtained from analysis of Figure 7. Thus the value of $k_{13}/k_{14} = 12.8$ may be deduced.

Figure 7 confirms the validity of Scheme II, particularly the 2-fold $TEOA$ vs. $Co(bpy)_3^{2+}$ competition (eq 12 vs. eq 11 and eq 14 vs. eq 13). An unanticipated and interesting result that emerges from this analysis is the rapidity of eq 13, oxidation of $Co(bpy)_3^{2+}$ by $TEOA^+$, the primary radical. As noted above, analysis of the data in Figure 7 gives $k_{13}/k_{14} = 12.8$. Neither k_{13} nor k_{14} has been measured in the 50% aqueous acetonitrile medium, but it is known that $k_{14} = (3.3 \pm 0.5) \times 10^6 M^{-1} s^{-1}$ in water ($\mu = 0.5 M$).²⁶ If this value for k_{14} is used in the 50% aqueous acetonitrile medium, then k_{13} is estimated as $4.2 \times 10^7 M^{-1} s^{-1}$. The only previously reported rate constant for oxidation by $TEOA^+$ is that

of $3 \times 10^9 M^{-1} s^{-1}$ for reaction with the much stronger reductant methylviologen radical ($E^\circ = -0.45 V$). The rapid oxidation of $Co(bpy)_3^{2+}$ by $TEOA^+$ indicates that the $TEOA^+/TEOA$ reduction potential is considerably more positive than $+0.30 V$ (the $Co(bpy)_3^{3+/2+}$ E°). The kinetics observed with the RuL_3^{3+} and OsL_3^{3+} oxidants are consistent with a value of $\sim +0.9 V$, which is similar to that estimated by Lehn and Sauvage.²⁹

An additional test of the mechanism in Scheme II is provided by the pH dependence of the hydrogen yields (Table VIII). As long as H_2 formation (eq 17) is sufficiently rapid, the only pH dependence predicted arises through the $TEOA-TEOAH^+$ equilibrium and the ensuing changes in the $TEOA$ to $Co(II)$ ratio. As is shown in Figure 8, such is the case below $pH \sim 8.4$; the experimental points (Table VIII) fall on the curve calculated from eq 18.

For 50% aqueous CH_3CN the limiting H_2 yield, 0.29 ± 0.01 , and the $Ru(III)-Co(I)$ yield, 0.27 ± 0.02 from flash photolysis, are identical within experimental error as is required for eq 8–17 if eq 16 is stoichiometric. This system thus appears limited (under optimum conditions) by the magnitude of Y_{ox} . Preliminary observations (see supplementary material, Tables VI–VIII) indicate the optimum H_2 yield in a purely aqueous medium to be about 10 times smaller. The solvent dependence of Y_{ox} is of some interest. In terms of Scheme I, Y_{ox} is given by

$$Y_{ox} = \frac{k_{23}k_{34}}{(k_{23} + k_{red}' + k_{en}') (k_{30}' + k_{34}) + k_{32}(k_{red}' + k_{en}')} \quad (19)$$

Since the cage-escape yield ϕ_{cage} is $k_{34}/(k_{30}' + k_{34})$, the yield of separated $Ru(III)$ and $Co(I)$ is also given by

$$Y_{ox} = f_{ox}\phi_{cage} \quad (20)$$

where $f_{ox} = k_{ox}/k_q$ and k_{ox} and k_q are given in eq 7. Thus Y_{ox} reflects the relative values of k_{ox} , k_{red}' , and k_{en}' and of k_{34} and k_{30}' . Since all of the rate constants are expected to be medium dependent, it is not feasible to address the Y_{ox} differences at a quantitative level at this time. It is worth noting, however, that k_{34} is expected to be greater in the lower viscosity acetonitrile mixture than in the purely aqueous solution, thereby promoting cage escape over "back-reaction" in the acetonitrile medium. An additional factor favoring cage escape in this system is the fact that the $Co(I)-Ru(III)$ back-reaction lies in the inverted region. For reactions in the inverted region the solvent dependence of the rate is such that k_{30} (within the *close contact* successor complex) is smaller in acetonitrile than in water, facilitating cage escape in the mixed solvent.³⁰

The sensitizer dependence of the H_2 yields in 50% acetonitrile may also be discussed in terms of Schemes I and II and eq 19 and 20. Provided that $k_{12}[TEOA] \gg k_{11}[Co(bpy)_3^{2+}]$ (note that L now varies) and that $k_{14}[TEOA] \gg k_{13}[Co(bpy)_3^{2+}]$, the variation of ϕ_{H_2} with sensitizer will reflect variations of Y_{ox} . With $[TEOA]/[Co(bpy)_3^{2+}] = 150$ the H_2 quantum yields determined were 0.12, 0.028, 0.23, and 0.23 for $L = 5-Clphen$, $phen$, $4,7-(CH_3)_2phen$, and $3,4,7,8-(CH_3)_4phen$, respectively. As noted above, for $L = 4,7-(CH_3)_2phen$, $k_{12}/k_{11} = 0.24$ and $k_{14}/k_{13} = 0.078$. Since the latter ratio is independent of RuL_3^{2+} , $TEOA^+$ rearrangement to $TEOA^+$ (eq 14) is $>90\%$ efficient for all the sensitizers in the above experiments. In addition, in view of the k_{11} magnitude (Table VI) and the fact that $TEOA-ML_3^{3+}$ reduction rate constants (k_{12}) exhibit a normal driving-force dependence,²⁸ k_{12}/k_{11} should be >0.1 for all the sensitizers used. Thus the ϕ_{H_2} values for the $phen$ and methylated $phen$ derivatives provide a measure of Y_{ox} . From the calculations presented in Figure 4, f_{ox} is 0.00, 0.12, 0.78, and 0.92 (same RuL_3^{2+} order as above), which, with the exception of 5-Clphen, discussed below, reflects remarkably well the relative ϕ_{H_2} values. In fact, the ratio of ϕ_{H_2} (measured) to f_{ox} (calculated) is 0.26 ± 0.03 , suggesting that ϕ_{cage} is rather similar (0.26 ± 0.03) for all three systems. Thus

(29) Lehn, J. M.; Sauvage, J. P. *Nouv. J. Chim.* **1977**, *1*, 449.

(30) Brunschwig, B. S.; Ehrenson, S.; Sutin, N. *J. Am. Chem. Soc.* **1984**, *106*, 6858.

Table X. Comparison of RuL₃²⁺-Sensitized Water-Photoreduction Systems^a

added components	pH	primary products (P _{el})	Y _{el}	φ _{H₂}	nφ _{H₂} /Y _{el} ^b	ref
(1) MV ²⁺ , EDTA, Pt	4	RuL ₃ ³⁺ + MV ⁺	0.25	0.13 ^c	0.5	26b, c
(2) Co(sep) ³⁺ , EDTA, Pt	4	RuL ₃ ³⁺ + Co(sep) ²⁺	0.51	0.13 ^{c,d}	0.25	26d
(3) Rh(bpy) ₃ ³⁺ , TEOA, Pt	8	RuL ₃ ³⁺ + RhL ₃ ²⁺	0.15	0.11 ^c	0.7	26a
(4) Et ₃ N, Pt (25% CH ₃ CN)		RuL ₃ ⁺ + Et ₃ N ⁺	≥0.2	0.44 ^{c,e}		31
(5) Eu(II), Co ^{II} (MAC)	5	RuL ₃ ⁺ + Eu(III)	1.0	0.05	0.02	27
(5) HAS ⁻ , Co ^{II} (MAC)	5	RuL ₃ ⁺ + HAS [•]	0.5	5 × 10 ⁻⁴	0.001	27
(6) HAS ⁻ , Co(bpy) _n ²⁺	5	RuL ₃ ⁺ + HAS [•]	0.5	0.03	0.12	2, 3
(7) Co(bpy) ₃ ²⁺ , TEOA (50% CH ₃ CN)	8	RuL ₃ ³⁺ + Co(bpy) ₃ ⁺	0.27	0.29	1.0	f

^aSee original reference for RuL₃²⁺ used. ^bThe stoichiometric factor *n* is equal to 1 or 2, depending on the nature of the subsequent reactions. ^cHeterogeneous H₂ formation catalyzed by platinum. ^dThe value reported in ref 26d has been corrected for the fraction of *RuL₃²⁺ not quenched. ^eL = 4,4'-dicarboxy-2,2'-bipyridine diisopropyl ester. ^fThis work.

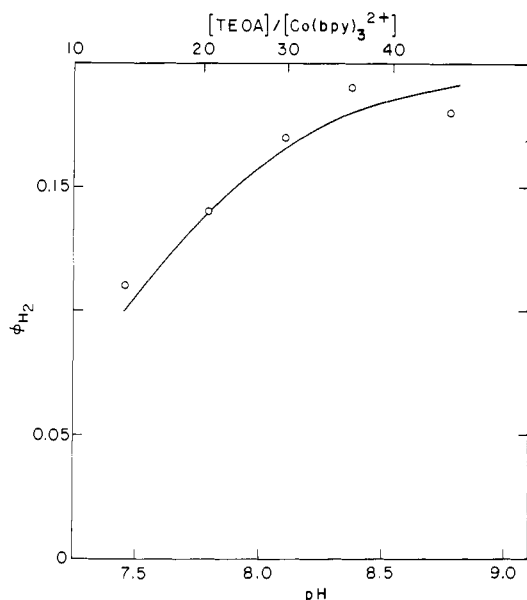


Figure 8. Variation of quantum yield for H₂ formation with pH at constant total triethanolamine concentration (Table VIII). The curve is calculated from eq 18 by using parameters given in the text.

this analysis strongly suggests that for these three sensitizers (L = phen, 4,7-(CH₃)₂phen, and 3,4,7,8-(CH₃)₄phen) the common photoreduction mechanism given in Scheme II is operative. Furthermore, it appears that all three systems are limited by low cage-escape yields (0.2–0.3) and that the variations among them are largely due to the competition between energy-transfer and oxidative electron-transfer quenching paths. The Ru(5-Clphen)₃²⁺ system provides the exception to the above conclusion. From Figure 4 it is evident that for this sensitizer *f*_{ox} ≈ 0, yet φ_{H₂} ≈ 0.1. This discrepancy leads us to consider alternative mechanisms for Ru(5-Clphen)₃²⁺. Preliminary work indicates that, in contrast to the phen and (CH₃)phen sensitizers, *Ru(5-Clphen)₃²⁺ is quenched by triethanolamine. Thus a reductive quenching pathway (Q = D = TEOA) as found with ascorbate ion (see eq 2a,b) is implicated. Additional mechanistic studies with Ru(5-Clphen)₃²⁺ are in progress.

Comparisons with Other Photoreduction Systems. In recent years a number of water photoreduction systems employing RuL₃²⁺ sensitizer have been developed.^{2,3,26,27,31} These are summarized in Table X. All require a “sacrificial” electron donor—EDTA, triethylamine, ascorbate, or triethanolamine. As mentioned in the introduction, the photochemical reaction may involve either excited-state oxidation forming RuL₃³⁺ or excited-state reduction to give RuL₃⁺. The primary photoproducts (P_{el}) are listed in the third column of the table. The yield of primary electron-transfer products Y_{el} (fourth column) imposes an upper limit on the H₂ yield for the system. For example, in the TEOA

((3) and (7)), Et₃N (4), and probably also the EDTA ((1) and (2))^{26b} systems, φ_{H₂} ≤ Y_{el} because of the production of secondary reducing radicals (see above and eq 14 and 16). Consequently, in these systems 1 mol of H₂ can, in principle, be produced per mol of (separated) primary products. On the other hand, in systems 5 and 6 where ascorbate or Eu²⁺ is the electron donor, φ_{H₂} ≤ Y_{el}/2 because secondary reducing radicals are not produced and 2 mol of primary products is needed to produce 1 mol of hydrogen. Just as Y_{el} describes the photochemical efficiency, nφ_{H₂}/Y_{el} measures the chemical efficiency of the subsequent reactions culminating in H₂ production. It is evident that the chemical efficiencies of the heterogeneous systems ((1)–(4)) can be quite high. Both the MV²⁺ (1) and Rh(bpy)₃³⁺ (3) systems are essentially limited only by the yields of separated electron-transfer products. Our earlier work with homogeneous systems 5 and 6 showed these to be subject to poor chemical efficiencies. By contrast, the present Co(bpy)₃²⁺ system 7 exhibits practically unit chemical efficiency. Interestingly, both systems 6 and 7 involve the common H₂-forming intermediate Co(bpy)₃⁺ (and Co(bpy)₃H²⁺). At pH 8 these react quantitatively to give H₂ and Co(bpy)₃²⁺. In the pH 5 ascorbate solutions, H₂ yields should also be quite high. However, in photochemical system 6, the relatively long-lived ascorbate radical oxidizes Co(I) competitively with H₂ formation (at pH < 5, bpy rather than H₂O reduction is favored).³ Thus the great contrast in the efficiencies of the two Co(bpy)_n²⁺-based systems is actually due to the free-radical chemistry of the sacrificial donors, and the rearrangement of the primary TEOA[•] radical (eq 14) is crucial to the high yield in system 7.

Conclusion

The reduction potentials of CoL₃^{3+/2+} and CoL₃^{2+/+} couples lie in the range +0.16 to +0.50 and –0.83 to –1.07 V, respectively. Thus from thermodynamic considerations, CoL₃²⁺ complexes may either reduce or oxidize the RuL₃²⁺ excited states. However, analysis of the quenching profile for *RuL₃²⁺–Co(bpy)₃²⁺ reactions indicates oxidative quenching of *RuL₃²⁺ (yielding Ru(III) and Co(I)) to be the only significant electron-transfer process. The reductive process (to yield RuL₃⁺ and Co(III)) is kinetically negligible because of the low CoL₃^{2+/3+} electron-exchange rate and because of the poor electronic factor for the reaction. In addition, energy-transfer quenching by Co(bpy)₃²⁺ is significant, reflecting a higher electronic factor for this process than is found for energy transfer from *RuL₃²⁺ to other cobalt(II) complexes. With L = 4,7-(CH₃)₂phen, the Co(bpy)₃²⁺–RuL₃²⁺ excited-state electron transfer to given Co(bpy)₃⁺ and RuL₃³⁺ results in the formation of H₂ in relatively high yield. The chemical efficiency of this homogeneous system is low at high [Co(bpy)₃²⁺]/[TEOA] ratios because of competitive reactions of Co(bpy)₃²⁺ with RuL₃³⁺ and with the triethanolamine cation radical; the Co(bpy)₃³⁺ produced in these reactions oxidizes the H₂ precursor Co(bpy)₃⁺. By contrast, at high triethanolamine concentrations the H₂ yield is limited only by the efficiency of primary product separation (cage-escape yield).

Acknowledgment. We thank M. Chou and Dr. D. Mahajan, who prepared some of the samples used in these studies, and E.

(31) (a) DeLaive, P. J.; Whitten, D. G.; Gianotti, C. *Adv. Chem. Ser.* **1979**, No. 173, 234. (b) DeLaive, P. J.; Sullivan, B. P.; Meyer, T. J.; Whitten, D. G. *J. Am. Chem. Soc.* **1979**, *101*, 4007.

Norton, who performed much of the analytical work. This research was carried out at Brookhaven National Laboratory under Contract DE-AC02-76CH00016 with the U.S. Department of Energy and supported by its Division of Chemical Sciences.

Supplementary Material Available: Medium effects on quenching rate constants, and H₂ yields as a function of sensitizer, solvent, donor, etc. (8 pages). Ordering information is given on any current masthead page.

Metal Ion Promoted Elimination Reactions. Conversion of β -Hydroxy α -Amino Acids to α -Imino Acids

E. K. Chong,[†] J. MacB. Harrowfield,[‡] W. G. Jackson,[§] A. M. Sargeson,^{*†} and J. Springborg[⊥]

Contribution from Research School of Chemistry, Australian National University, Canberra A.C.T., 2601 Australia, Department of Physical and Inorganic Chemistry, University of Western Australia, Nedlands W.A., 6009 Australia, and Chemistry Department, University of New South Wales, Royal Military College, Duntroon A.C.T., 2601 Australia. Received April 18, 1984

Abstract: Base-catalyzed elimination reactions of *O*-acetyl- and *O*-sulfonylserine coordinated to cobalt(III) give rise to chelated 2-iminopropanoate. The reaction rates are first order in [OH⁻] and independent of buffer base concentration and are equal in magnitude to the methine proton exchange rates. Comparison with the rate of elimination for the free ligand, *O*-sulfonylserine, in base shows that coordination results in $\sim 10^7$ -fold increase in reactivity. For N,O-coordinated (*S*)-methionine, elimination of methanethiol is similarly facilitated, though in this complex the rate of methine proton exchange exceeds that of elimination by a factor of ~ 25 . Reaction mechanisms are discussed. The methyl group in chelated 2-iminopropanoate is deprotonated readily in base and the carbanion so generated reacts rapidly with electrophiles such as aldehydes.

Subtle control of the reaction pathways available to an organic substrate is one of the well-known consequences of complex formation with a metal ion. Recognition of the formal charge donation and acceptance involved in complexation leads to the anticipation that ligand nucleophilicity should be reduced while electrophilicity is enhanced^{1,2} and, in gross terms, metal ion catalysis can often be assessed in this way. However, detailed investigations of mechanism attest to the superficiality of this view,³ so that it is necessary in as many instances as possible to probe beyond the mere metal ion dependence of a process. One convenient means of so doing is to examine metal ion promoted reactions (occurring at a substitutionally inert metal ion center) where the ligand remains bound to the metal ion for the lifetime of the organic reaction.

Hydroxy amino acids and their derivatives have numerous biological and synthetic uses.⁴⁻⁶ Elimination processes are apparently involved in the enzymic conversion of, in particular, serine and its derivatives to other β -functionalized amino acids.⁷⁻⁹ The immediate product, dehydroalanine, is either captured by a nucleophile to give a new amino acid or it rearranges to the iminopyruvate (2-iminopropanoate), which then decays further to ammonia and pyruvic acid (Scheme I).

Some of these processes involve pyridoxal to trigger the elimination, others do not. One such pyridoxal free system has been described by Tudball et al. for the elimination of sulfate ion from *O*-sulfonylserine to produce iminopyruvate and hence ammonia and pyruvate ion.⁹ The question which arises for these latter systems is what triggers the elimination process. This paper examines the possibility of metal ions activating the elimination since it is well-known that the methine proton of α -amino acids becomes more acidic on chelation of the amine and carboxylate groups to some metal ions.⁵ Certainly, simple metal ion pyridoxal catalyzed elimination reactions of serine and threonine (and their derivatives) have been observed, though often only in conditions where the anticipated immediate reaction products were not detected.¹⁰

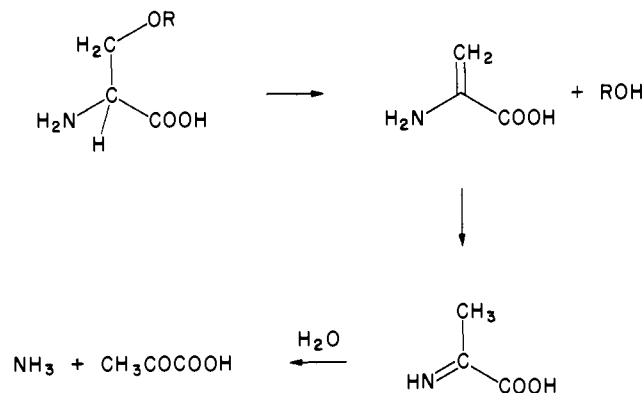
[†] Australian National University.

[‡] University of Western Australia.

[§] University of New South Wales.

[⊥] Royal Agricultural and Veterinary University, Copenhagen.

Scheme I



The facile β -elimination of the nitro group in chelated nitroalanine to give a stable Co(III)-pyruvate-imine chelate¹¹ implied

(1) These effects have been widely discussed and analyzed. See, for example: Jones, M. M.; Hix, J. E. In "Inorganic Biochemistry"; Eichhorn, G. L., Ed.; Elsevier: Amsterdam, 1973; Chapter 13, Vol. 1.

(2) Nugent, W. A.; McKinney, R. J.; Kasowski, R. V.; Vancatledge, F. A. *Inorg. Chim. Acta* **1982**, *65*, L91-L93.

(3) Again, this issue has been widely discussed. See, for example, ref 1. Also: Buckingham, D. A.; Keene, F. R.; Sargeson, A. M. *J. Am. Chem. Soc.* **1974**, *96*, 4981-4983 and references therein.

(4) Greenstein, J. P.; Winitz, M. "The Chemistry of the Amino Acids"; Wiley: New York, 1961; Vol. 3, Chapter 49. Meister, A. "Biochemistry of the Amino Acids"; Academic Press: New York, 1957.

(5) Williams, D. H.; Busch, D. H. *J. Am. Chem. Soc.* **1965**, *87*, 4644-4645. Terrill, J. B.; Reilly, C. N. *Inorg. Chem.* **1966**, *5*, 1988-1996. Buckingham, D. A.; Marzilli, L. G.; Sargeson, A. M. *J. Am. Chem. Soc.* **1967**, *89*, 5133-5138.

(6) Bose, A. K.; Manhas, M. S.; Vincent, J. E.; Gala, K.; Fernandez, J. F. *J. Org. Chem.* **1982**, *47*, 4075-4081.

(7) Davis, L.; Metzler, D. E. In "The Enzymes", 3rd ed.; Boyer, P. D., Ed.; Academic Press: New York, 1972; Vol. VII, Chapter 2.

(8) Runeckles, V. C.; Conn, E. E., Eds. "Recent Advances in Phytochemistry"; Academic Press: New York, 1974; Vol. 8, Chapter 5.

(9) O'Neill, J. G.; Tudball, N. *Biochim. Biophys. Acta* **1976**, *429*, 616-623 and references therein.

(10) Marcello, J. A.; Martell, A. E. *J. Am. Chem. Soc.* **1982**, *104*, 3441-3447 and references therein.